

Synthesis and Characteristics of Different Compositions of $\text{Nd}_{1-x}\text{Ba}_x\text{MnO}_3$ Nano-crystalline Perovskite

Dr. Jessica Chocha

Department of Physics, Government Science College, Junagadh, Gujarat, India
Email – jessicaphysics@gmail.com

Abstract: High purity powders of the compositions, $\text{Nd}_{1-x}\text{Ba}_x\text{MnO}_3$ (NBMO), ($x = 0.1 - 0.5$) were synthesized using the citrate pyrolysis process. Using high purity chemicals of Nd_2O_3 , BaCO_3 , MnO_2 , HNO_3 , citric acid and ethylene glycol, prepared solution was kept for heating under continuous stirring until gel was obtained. Then it was converted in resin by giving more heating in an oven. The resin was pulverized and calcined at various temperatures to obtain various NBMO nanoparticles. These compositions were characterized by X-ray diffraction (XRD), Atomic force microscopy (AFM). The formation of monophasic material and absence of secondary phase were confirmed through XRD. The samples calcined at 900 °C for 2h are polycrystalline in nature and with average crystallite sizes ~ 17 - 25 nm. Higher temperature sintered samples have orthorhombic perovskite structure. The NBMO compositions show a homogeneous grain size in nanometer scale as shown by AFM studies.

Key Words: CMR, Sol-gel method, Perovskite, Nanostructured.

1. INTRODUCTION:

The physical properties of CMR compounds are influenced by several parameters [1]. The chemical composition mainly affects the magnetic behaviour and the magnetic and electrical transition temperatures. The synthesizing methods are very important to obtain the polycrystalline with special microstructure. In general, these oxides are synthesized at high temperatures using a standard ceramic technique, and hence the microstructure is difficult to be governed. Chemical preparation methods called “soft chemistry processing” such as sol-gel [2, 3] and co-precipitation methods [4, 5] have been introduced to synthesize the CMR oxides. All these methods maintain the metal precursors in a highly dispersed state, and hence favour more homogenous powders at relatively low temperatures. Most of the studies done on Ba-substituted compounds are lanthanum barium manganites [6]. In this paper, we have synthesized a different barium concentration substituted neodymium compound, $\text{Nd}_{1-x}\text{Ba}_x\text{MnO}_3$ and the results of such an investigation are presented here.

Recently, modification of the properties of nanosized perovskite has aroused much interest [4-6]. There has been less work on Ba-containing manganites [7]. The physical properties are usually dependent on their preparation routes [8]. Furthermore, the nanosized particles may lead to some interesting magnetic and electronic properties than the bulk materials [9]. Chemical methods give the ability to produce powders with exceptionally small particle size in the nanometer range. A variety of methods have been developed to prepare manganite perovskites nanoparticles viz. sol-gel route [10], co-precipitation [11], molten salt method [12], hydrothermal synthesis [13], auto combustion process [14], micro emulsion [15] etc. to synthesize fine or ultra fine particles with desired size and narrow distribution. We successfully overcome this barrier by utilizing a simple, versatile and easy chemical process. In this paper, we present the results on the successful synthesized different compositions of $\text{Nd}_{1-x}\text{Ba}_x\text{MnO}_3$ ($x = 0.1 - 0.5$) nanoparticles by simple citrate pyrolysis method at relatively low temperatures.

2. METHOD:

The $\text{Nd}_{1-x}\text{Ba}_x\text{MnO}_3$ ($x = 0.1 - 0.5$) compositions were prepared using the citrate pyrolysis process. Here high purity starting materials viz. neodymium oxide (99.9%), barium carbonate (99.9%) and manganese dioxide (99.9 %) including citric acid (99.9 %), nitric acid and ethylene glycol were used. In typical procedure, Nd_2O_3 , BaCO_3 and MnO_2 were mixed thoroughly for 5-10 minutes using an agate mortar and then the resulting precursor was dissolved in nitric acid (HNO_3) solution at about 80 °C. After that 0.3 mole citric acid and 0.1 mole of ethylene glycol were dissolved in de-ionized water separately and then mixed with the above nitric acid (HNO_3) solution under continuous stirring, the resulting solution was heated at 80 – 90 °C until it turned into brown colored gel. Then dark brown resin was obtained from the brown gel by drying the same at 150 °C for 1440 minutes in an oven. Finally, the resulting resin was pulverized and then calcined at various temperatures to optimize synthesis condition of the NBMO nanoparticles. X-ray diffraction (XRD) patterns were collected in the range 20 - 80° with 0.02° steps using $\text{CuK}\alpha$ radiation with PANalytical X'pert Pro-diffractometer Model PW3209. The average crystallite sizes were estimated using peak broadening through Scherrer formula. Surface morphology and the estimation of grain sizes were carried out for all

samples using an atomic force microscope (AFM - Nanoscope E from Digital Instruments USA). The electrical resistance and magneto-resistance (MR) measurements of pelletized samples were performed using physical properties measurements system (PPMS), under applied different magnetic fields.

3. DISCUSSION :

The XRD results of the prepared NBMO compositions sintered at 200 °C, 300 °C, 600 °C, and 900 °C for 2 h are shown in figure 1 (a - e) respectively. When the powders calcined at 200 & 300 °C, for 2 h, the resultant NBMO compositions show purely amorphous phase as shown in figure 1 (a-e). When calcination temperature is increased up to 600 °C, the crystalline phase was produced in each case but some minor unwanted peaks were found in the compositions. The figure shows the pure phase of neodymium-barium manganite with no extra impurity phase or phases in all the NBMO compositions calcined at 900 °C. The diffraction peaks in all NBMO samples calcined at 900 °C for 2 h, show sharper profiles resulting from the combination of crystallization/ordering processes and gradual grain growth, which are in accordance to the orthorhombic symmetry reduction of this perovskite. The crystallite sizes of the synthesized samples were estimated through the Debye-Scherrer equation using XRD peak broadening and found in the range of 17 - 25 nm for all NBMO sintered at 900 °C. The diffraction peaks for all the NBMO sintered at 900 °C show sharper profiles resulting from the combination of crystallization/ordering process and gradual grain growth, which are in accordance to the orthorhombic symmetry reduction of this perovskite with the same space group Pnma (No. 62).

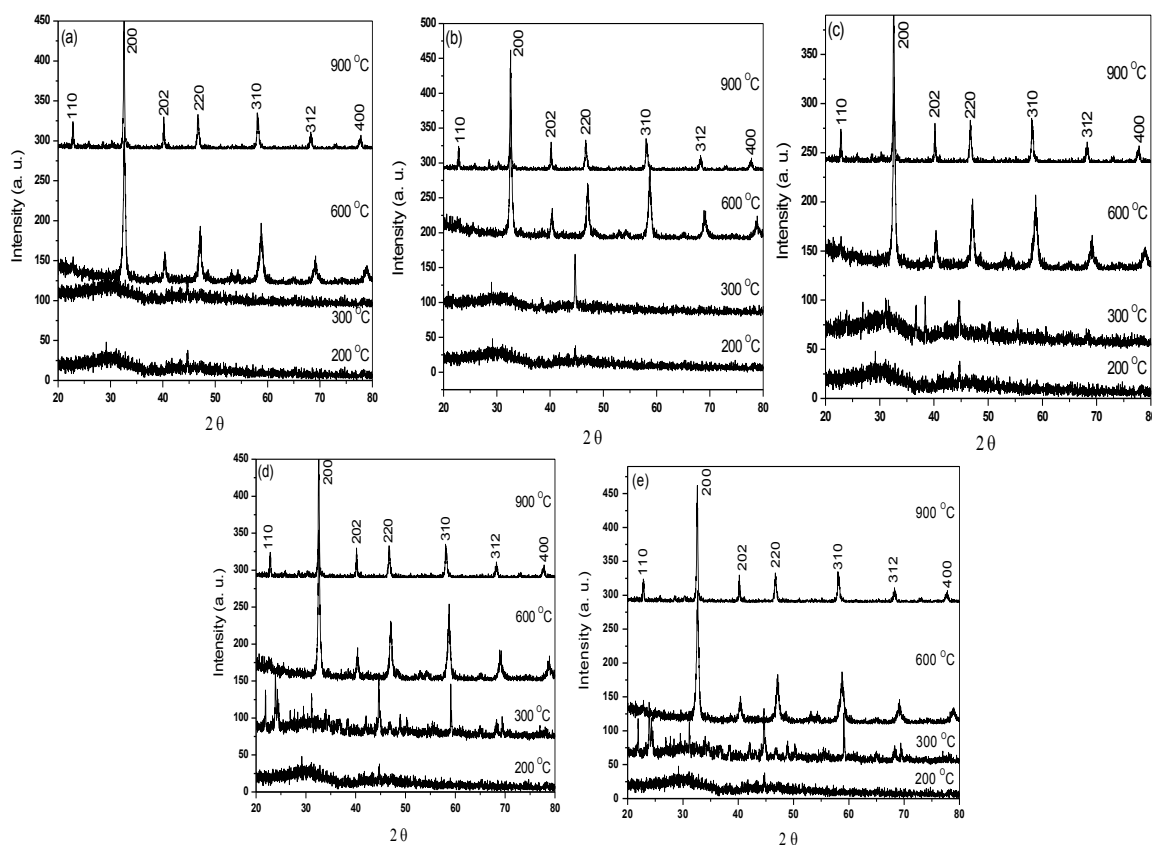


Figure 1: XRD plots of (a) $\text{Nd}_{1-x}\text{Ba}_x\text{MnO}_3$ ($x = 0.1$), (b) $\text{Nd}_{1-x}\text{Ba}_x\text{MnO}_3$ ($x = 0.2$), (c) $\text{Nd}_{1-x}\text{Ba}_x\text{MnO}_3$ ($x = 0.3$), (d) $\text{Nd}_{1-x}\text{Ba}_x\text{MnO}_3$ ($x = 0.4$) and (e) $\text{Nd}_{1-x}\text{Ba}_x\text{MnO}_3$ ($x = 0.5$) compositions sintered at 200 °C, 300 °C, 600 °C, and 900 °C, 2 h.

The surface morphology of the different NBMO compositions sintered at 900 °C has been studied by contact mode atomic force microscope (AFM). Atomic force microscopy (AFM) images of the different NBMO compositions in pellet forms are shown in figure 2 (a - e). The two dimensional (2D) AFM images of NBMO ($x = 0.1 - 0.5$) sintered at 900 °C for 2 h, show uniformly clear grain formation with a spherical shape. Analysis of the AFM images reveals that crystalline blocks have a narrow size distribution with in a nano-meter range. The obtained average grain size and surface roughness values for NBMO ($x = 0.1 - 0.5$) sintered at 900 °C are 45, 43, 41, 39 & 35 nm and 35, 38, 41, 43 & 51 respectively. From these values it is concluded that as the concentration of Barium increases, average grain size decreases and surface roughness increases.

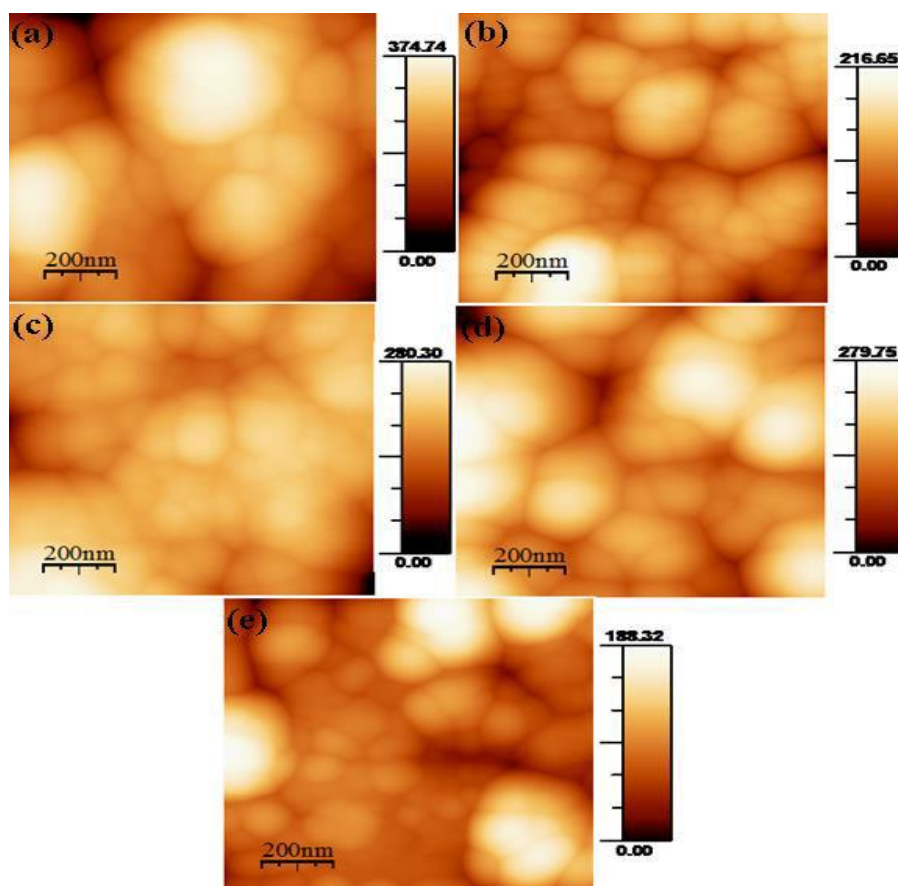


Figure 2: Atomic force microscopy (AFM) images of (a) $\text{Nd}_{1-x}\text{Ba}_x\text{MnO}_3$ ($x = 0.1$), (b) $\text{Nd}_{1-x}\text{Ba}_x\text{MnO}_3$ ($x = 0.2$), (c) $\text{Nd}_{1-x}\text{Ba}_x\text{MnO}_3$ ($x = 0.3$), (d) $\text{Nd}_{1-x}\text{Ba}_x\text{MnO}_3$ ($x = 0.4$) and (e) $\text{Nd}_{1-x}\text{Ba}_x\text{MnO}_3$ ($x = 0.5$) compositions sintered at 900°C , 2 h.

The temperature dependence of the electrical resistivity $\rho(T)$ measured in absence and different presence magnetic fields (1 T, 5 T, 9 T & 14 T) are shown in figure 3 (a - e).

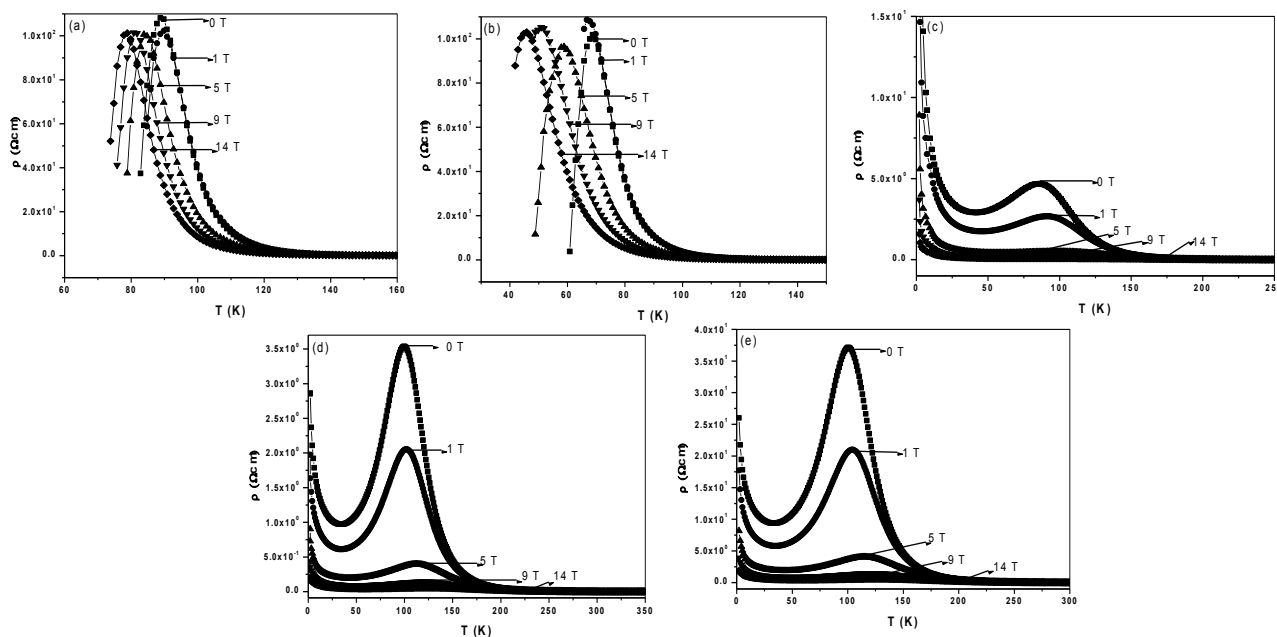


Figure 3: The temperature dependence resistivity of the (a) $\text{Nd}_{1-x}\text{Ba}_x\text{MnO}_3$ ($x = 0.1$), (b) $\text{Nd}_{1-x}\text{Ba}_x\text{MnO}_3$ ($x = 0.2$), (c) $\text{Nd}_{1-x}\text{Ba}_x\text{MnO}_3$ ($x = 0.3$), (d) $\text{Nd}_{1-x}\text{Ba}_x\text{MnO}_3$ ($x = 0.4$) and (e) $\text{Nd}_{1-x}\text{Ba}_x\text{MnO}_3$ ($x = 0.5$) compositions sintered at 900°C , 2 h at various magnetic fields.

Figure 3 (a - e) shows the temperature dependence resistivity under the different magnetic fields (0 T, 1 T, 5 T, 9 T & 14 T) for the NBMO ($x = 0.1 - 0.5$) samples sintered at 900°C , 2 h. In the absence of magnetic field, all the NBMO compositions have a resistivity maximum value (T_{MI}) in the temperature dependence of the resistivity near T_c .

as shown in figure 3 (a - e). The peak in resistivity becomes broader and shifts to higher temperatures for $x = 0.3 - 0.5$ as the magnetic field increases. Here for $x = 0.3 - 0.5$, resistivity upturn behaviour was found after T_{\min} , while for $x = 0.1 - 0.2$ samples, no upturn behaviour and T_{\min} was found. Because of very high value of low temperature resistance in the limit of measurability of the PPMS system and unavailability of enough low temperature, the upturn and complete metallic behaviour was not possible to study. For NBMO, $x = 0.3, 0.4$ & 0.5 (figure. 3(c), (d) & (e)), the resistivity can be divided into different regions between 20 and 250 K which correlates well with the two magnetic phase transitions. With decreasing temperature the resistivity increases monotonically as in the case of an insulator/semiconductor ($d\rho/dT < 0$). The resistivity reaches maximum and then decreases rapidly as temperature is decreased to ~ 32 K. This metallic behaviour is induced by the ferromagnetic ordering that drastically enhances the electron hopping rate for Mn^{+3} , Mn^{+4} which strongly depends on the relative orientation of the Mn ions [15]. The low temperature below around 32 K, increase in resistivity can be due to the tunnelling states resulting from the grain boundaries.

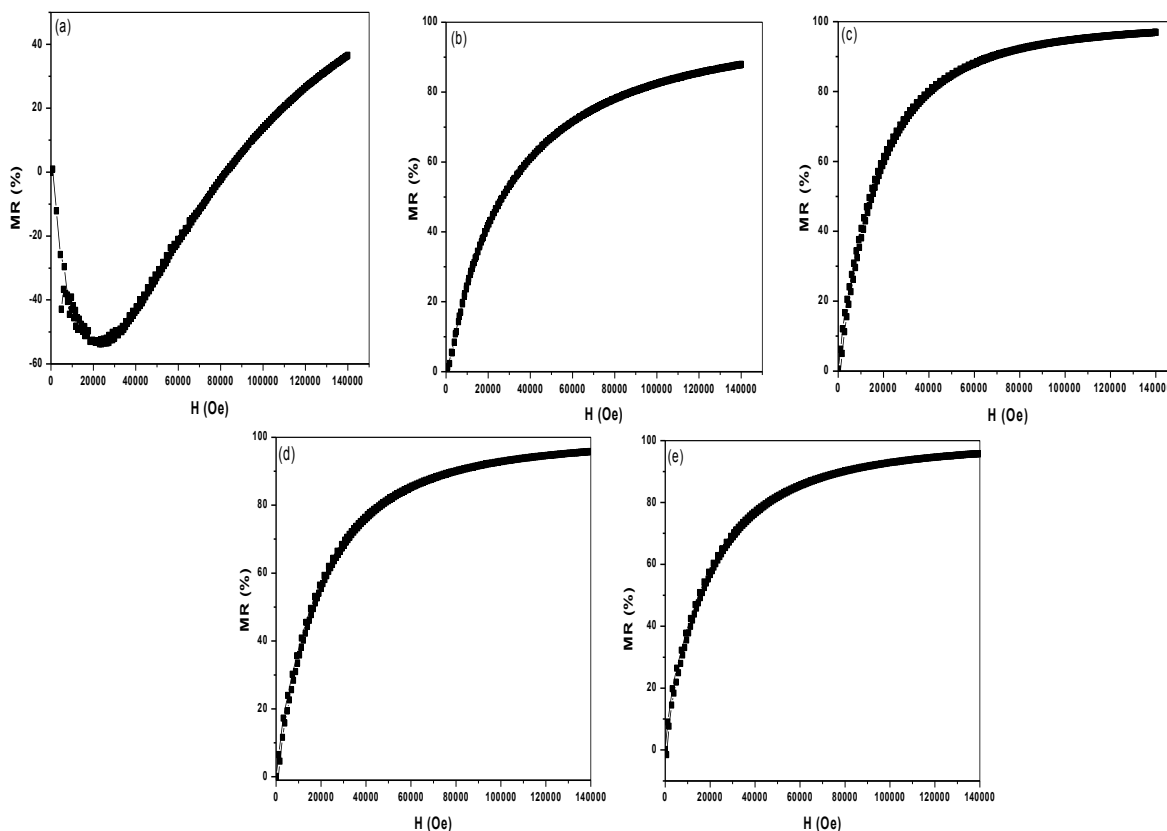


Figure 4: The isotherm magnetoresistance at 50 K of the (a) $Nd_{1-x}Ba_xMnO_3$ ($x = 0.1$), (b) $Nd_{1-x}Ba_xMnO_3$ ($x = 0.2$), (c) $Nd_{1-x}Ba_xMnO_3$ ($x = 0.3$), (d) $Nd_{1-x}Ba_xMnO_3$ ($x = 0.4$) and (e) $Nd_{1-x}Ba_xMnO_3$ ($x = 0.5$) compositions sintered at 900 °C, 2 h.

In the figure 4 (a) – (e), the results of isotherm magnetoresistance at 50 K measurements on NBMO ($x = 0.1 - 0.5$) compositions under the magnetic field up to 0 – 14 kOe are depicted. From the curves in figure 4 (b - e), it is concluded that for below 4 kOe region; as the field increases, MR % increases rapidly and then above 4 kOe; rate of increase decreases and goes towards saturation. But for NBMO ($x = 0.1$), the MR value first decreases negatively up to 2 kOe and then increases towards oppositely.

4. CONCLUSION:

In summary, a barium-substituted neodymium manganite, NBMO ($x = 0.1 - 0.5$) compositions were successfully synthesized at 900 °C for a duration of 2 h by using citrate pyrolysis process. The major advantage of this method is the formation of chemically pure and crystalline perovskite at relatively lower temperature and time duration. This chemical preparation method has potential advantages over the ceramic route, not only for achieving homogeneous mixing of components on the atomic scale easily, but also for controlling the microstructure effectively. The powder X-ray diffraction results of NBMO ($x = 0.1 - 0.5$) sintered at 900 °C confirmed the single phase nature with no detectable impurity phase or phases in all the NBMO compositions. XRD results show that NBMO sintered at 900 °C crystallizes in an orthorhombic structure with the space group of Pnma. These compositions also show the crystallite size in the range of 17 - 25 nm. The crystallite size values obtained from AFM images are also in nanometer range and clear grain morphology was found in all the compositions. The resistivity data of the NBMO ($x = 0.3$

- 0.4) sintered at 900 °C compositions show complete CMR effect and the resistivity decreases with the increase in the applied magnetic field. These compounds also show maximum MR value around 1000. The NBMO compounds exhibit CMR related magnetic phase transitions at $T_p = 100$ K. The NBMO compounds exhibit two magnetic phase transitions with entire temperature $T_c = 115$ K and $T_{Nd} = 40$ K, where T_{Nd} is the onset temperature for the partial ordering of the Nd moments. The higher MR at very low temperature is probably associated with the re-entrant metal to insulator transition that accompanies the magnetic phase transition at T_{Nd} .

ACKNOWLEDGEMENT : Part of this work was performed using UGC-DAE consortium for scientific research Indore. Help from Dr. V. Ganesan is thankfully acknowledged for this measurement.

REFERENCES :

1. Leslie-Pelecky DL, Rieke RD *Chem Mater*, 8, 1773, (1996).
2. Skomski R *J Phys: Condens Matter* 15, R841, (2003).
3. Fu Y *Appl Phys Lett*. 77, 118, (2000).
4. Venkataiah G, Venugopal Reddy P *J Magn Magn Mater* 285, 343, (2005).
5. Venkataiah G, Kalyana Lakshmi Y, Prasad V, Venugopal Reddy P *J Nanoscience and Nanotech* 7, 2000, (2007).
6. Z. Jirak, E. Pollert, A. F. Andersen, J. C. Grenier, and P. Hagenmuller, *Eur J. Solid State Inorg. Chem.* 27, 421, (1990).
7. B. Raveau, A. Maignan, and V. Caignaert *J. Solid State Chem.* 117, 424, (1995).
8. M. Uehara, S. Mori, C. H. Chen, and S.-W. Cheong *Nature (London)* 399, 560, (1999).
9. P. G. de Gennes *Phys. Rev.* 118, 141 (1960).
10. R.D. Sa´nchez, J. Rivas, C. Va´zquez-Va´zquez, M.A. Lo´pez- Quintela, M.T. Cause, M. Tovar, S.B. Oseroff *Appl. Phys. Lett.* 68 134, (1996).
11. J.A.M. van Roosmalen, E.H.P. Cordfunke *J. Solid State Chem.* 110, 106. (1994).
12. J.A.M. van Roosmalen, P. van Vlaanderen, E.H.P. Cordfunke, W.L. Ijdo, D.J.W. Ijdo *J. Solid State Chem.* 114, 516, (1995).
13. B.C. Hauback, H. Fjellvag, N. Sakai *J. Solid State Chem.* 124, 43, (1996).
14. F. Gao, R.A. Lewis, X.L. Wang, S.X. Dou *J. Alloys Compd.* 347, 314 (2002).
15. P. Dura´n, D. Gutierrez, J. Tartaj, M.A. Bana´res, C. Moure *J. Eur. Ceram. Soc.* 22, 797–807 (2002).
16. Ziese, M. *Phys. Rev., B* 62, 1044, (2000).